

Spatially variable stage-driven groundwater-surface water interaction inferred from time-frequency analysis of distributed temperature sensing data

Kisa Mwakanyamale,¹ Lee Slater,¹ Frederick Day-Lewis,² Mehrez Elwaseif,¹ and Carole Johnson²

Received 30 December 2011; revised 20 February 2012; accepted 22 February 2012; published 20 March 2012.

[1] Characterization of groundwater-surface water exchange is essential for improving understanding of contaminant transport between aquifers and rivers. Fiber-optic distributed temperature sensing (FODTS) provides rich spatiotemporal datasets for quantitative and qualitative analysis of groundwater-surface water exchange. We demonstrate how time-frequency analysis of FODTS and synchronous river stage time series from the Columbia River adjacent to the Hanford 300-Area, Richland, Washington, provides spatial information on the strength of stage-driven exchange of uranium contaminated groundwater in response to subsurface heterogeneity. Although used in previous studies, the stage-temperature correlation coefficient proved an unreliable indicator of the stage-driven forcing on groundwater discharge in the presence of other factors influencing river water temperature. In contrast, S-transform analysis of the stage and FODTS data definitively identifies the spatial distribution of discharge zones and provided information on the dominant forcing periods (≥ 2 d) of the complex dam operations driving stage fluctuations and hence groundwater-surface water exchange at the 300-Area. **Citation:** Mwakanyamale, K., L. Slater, F. Day-Lewis, M. Elwaseif, and C. Johnson (2012), Spatially variable stage-driven groundwater-surface water interaction inferred from time-frequency analysis of distributed temperature sensing data, *Geophys. Res. Lett.*, 39, L06401, doi:10.1029/2011GL050824.

1. Introduction

[2] The natural contrasts in temperature between groundwater and surface water provide opportunities to use temperature to obtain both quantitative and qualitative information on groundwater-surface water exchange. Groundwater exhibits relatively constant temperature compared to surface water, e.g., stream temperatures vary annually on a range between 0°C and 25°C [Constantz *et al.*, 1994] whereas groundwater commonly exceeds the mean annual air temperature of the locality by 2 to 3 degrees [Bechert and Heckard, 1966] and varies little over the seasons. The use of fiber optic distributed temperature sensing (FODTS) allows continuous measurements of temperature in both time and space at a high spatiotemporal resolution, and can now be deployed with cable lengths up to thousands of meters, with temperature resolution

of 0.01°C for every meter, and with temporal resolution of fractions of a minute. FODTS has been used in a number of hydrological studies, especially in studies of groundwater-surface water exchange. For example, Selker *et al.* [2006a] used FODTS in fluvial systems to locate groundwater sources along a stream, whereas Lowry *et al.* [2007] used FODTS to identify spatial variability in groundwater discharge in wetland systems. FODTS produces rich temporal datasets suitable for both time series and time-frequency analysis, although, until recently, the benefits of this analysis of FODTS data have not been fully exploited.

[3] The Fourier transform has been used for spectral analysis of time series for decades. The lack of time localised information in the Fourier spectrum [Mansinha *et al.*, 1997a, 1997b] led to the development of more powerful methods that offer joint time-frequency representation of time series, e.g., the S-transform [Stockwell *et al.*, 1996]. Such transforms offer progressive resolution of both time and frequency. Time-frequency analysis of FODTS data therefore provides a means to better understand spatial and temporal variations of hydrological processes by examining the frequency content of those processes as a function of time. Henderson *et al.* [2009] demonstrated the use of time-frequency analysis of FODTS by using a wavelet transform to characterize the time-variable frequency content of a FODTS temperature time series and comparing it with a tidal level time series, in order to improve understanding of forcing mechanisms on aquifer-estuary exchange.

[4] In this study, we (1) demonstrate the use of time-frequency analysis to provide proxy indicators of exchange that are more reliable than parameters extracted from the time series alone, and (2) obtain spatial information on the strength of the stage-driven exchange in response to subsurface heterogeneity along a major river corridor where heterogeneity is believed to influence the exchange of Uranium contaminated groundwater with river water.

2. Field Site

[5] The 300-Area is located at the south end of the Hanford site, north of Richland, Washington (Figure 1a). Uranium contaminated groundwater in the 300-Area discharges into the Columbia River through the zone of groundwater-surface water exchange along the river corridor. The Integrated Field Research Challenge (IFRC) site has been established in the 300-Area to study field-scale contaminant mass transfer processes [Ma *et al.*, 2011]. Our study site is a 1.6-km long portion of the river corridor approximately centered on the IFRC. The hydrogeologic framework of the river corridor at the 300-Area is defined by

¹Department of Earth and Environmental Sciences, Rutgers University, Newark, New Jersey, USA.

²Branch of Geophysics, Office of Groundwater, U.S. Geological Survey, Storrs, Connecticut, USA.

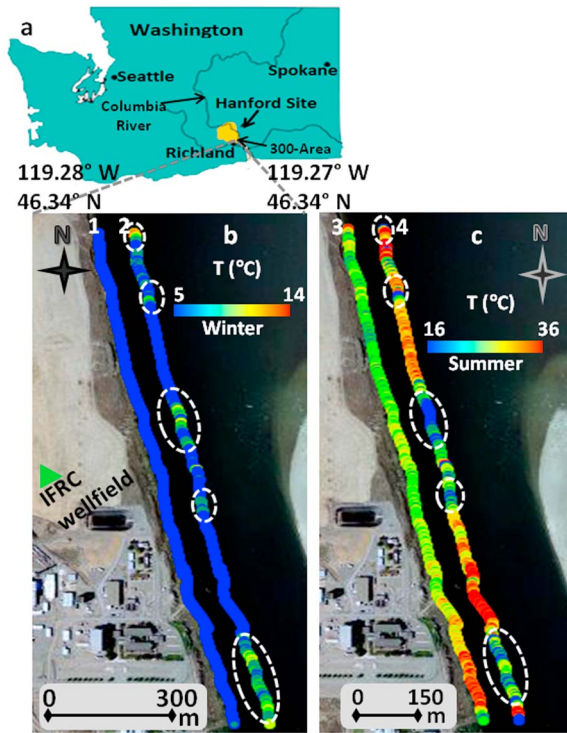


Figure 1. (a) Map of Washington State showing the location of Hanford Site in Richland, Washington, with the 300-Area located in the southeast. (b) Winter temperature distribution over 1.6 km of fiber-optic cable placed 2 m from shore, with the green triangle representing the IFRC well-field area. Temperature measurements at high river stage on 28 February 2009 (line 1). Temperature measurements at low river stage on 15 March 2009 (80 m offset for clarity) (line 2). (c) Summer temperature distribution over the fiber-optic cable. Temperature measurements at high river stage on 20 August 2009 (line 3). Temperature measurements at low stage on 3 August 2009 (80 m offset for clarity) (line 4). White dashed circles represent areas of focused groundwater-surface exchange. All color scales are linear.

an upper unconsolidated permeable aquifer (Hanford Formation) overlying a less permeable semi-consolidated and semi-confining unit (Ringold Formation). Geophysical imaging suggests that the thickness of the Hanford Formation ranges from 13.01 to 0.33 m along the 300-Area river corridor, being thicker towards the north, and thinning out in the south where the underlying Ringold Formation is in contact with the riverbed [Slater *et al.*, 2010].

[6] The Hanford Formation consists of unconsolidated sediments, pebble to boulder sized basalts and fine to coarse grained sand [Kunk and Narbutovskih, 1993] with a high hydraulic conductivity of ~ 2000 m/d [Williams *et al.*, 2007]. The Ringold Formation is divided into gravel dominated (upper) and mud dominated (lower) units [Newcomb, 1958]. The upper unit consists of cemented and compacted quartzitic gravels with mica rich silt and fine sand matrix [Lindberg and Bond, 1979] with hydraulic conductivity of 40–120 m/d [Williams *et al.*, 2007]. The lower unit has hydraulic conductivity of ~ 1 m/d [Williams *et al.*, 2007] and consists of silty-clay to silty-sand sediments [Tyler, 1992].

Focused exchange between groundwater and river water along the Columbia River corridor in the 300-Area is believed to be facilitated by buried channels of high permeability floodwater deposits locally incised below the Hanford-Ringold contact during low river stage [Lindberg and Bond, 1979]. These channels are believed to run both parallel and perpendicular to the river. Slater *et al.* [2010] found evidence of the paleochannels in waterborne electrical imaging surveys and temperature anomalies from FODTS datasets along the 300-Area river corridor. These results suggest that spatial variation in lithology along the Columbia River corridor is likely to exert a strong control on stage-driven focused groundwater discharge into the river. Direct evidence for focused exchange at the riverbed comes from uranium seeps identified at a number of locations (Spr-7–Spr-11) [Williams *et al.*, 2007] along the river corridor (Figure 2). Complex river stage fluctuations

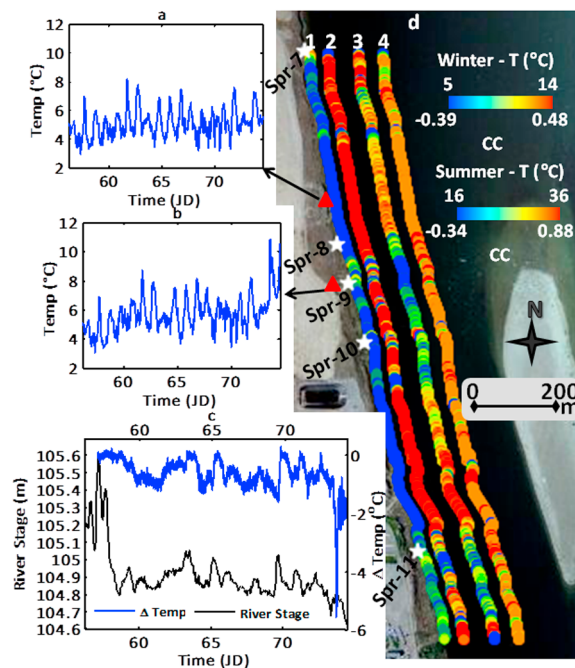


Figure 2. (a) Temperature distribution time series for an inferred non-exchange area. (b) Temperature distribution time series for a selected GDZ. (c) Interpolated river stage time series (black) and the difference in temperature between Figures 2b and 2c (blue). (d) Analysis of the complete FODTS cable, with labels at top as follows: temperature distribution for measurements at low stage on 15 March 2009 (line 1); correlation coefficient between temperature and river stage on 15 March 2009 (60 m offset) (line 2); temperature distribution for measurements at low stage on 3 August 2009 (130 m offset) (line 3); and correlation coefficient between temperature and river stage on 3 August 2009 (190 m offset) (line 4). White stars represent known uranium seeps (Spr-7–Spr-11) [Williams *et al.*, 2007]. Red triangles identify locations of time series for non-exchange versus exchange locations shown in Figures 2a and 2b, respectively. All color scales are linear; the top axis of the color bar is temperature, the bottom axis displays the correlation coefficient (CC): JD denotes Julian Day.

controlled by dam operations upstream of the 300-Area [Lindberg and Bond, 1979] impose a complex flow head boundary condition, regulating groundwater exchange and presumably influencing uranium transport via these seeps.

3. Methods

3.1. FODTS

[7] The FODTS method is based on measuring the travel time of a scattered or reflected laser pulse returned from points along the fiber optic cable. A portion of the transmitted energy is scattered back with wavelength less than (anti-Stokes) and higher than (Stokes) the original wavelength, as a result of (1) density changes in the fiber caused by electromagnetic forces from the passage of light (Brillouin Scattering) [Selker *et al.*, 2006b], and (2) loss/gain of energy exchange with electrons (Raman Scattering) [Selker *et al.*, 2006b]. The amplitude of the Raman anti-Stokes backscatter is linearly dependent on temperature. By measuring the ratio of the amplitude of the anti-Stokes to the Stokes backscatter, temperature can be recorded everywhere along the cable [Selker *et al.*, 2006a, 2006b].

3.2. S-Transform

[8] The S-transform is an extension of the windowed Fourier transform that was introduced and defined by Stockwell *et al.* [1996] as a time-frequency representation, whereby the local frequency spectrum is defined at each point along the time axis. This spectral localization is different from the wavelet transform [Mansinha *et al.*, 1997a] used to analyze FODTS data by Henderson *et al.* [2009] in that the S-transform preserves frequency-dependent resolution while simultaneously maintaining the direct relationship with the Fourier spectrum through time-averaging [Stockwell *et al.*, 1996].

[9] The 1-D S-transform is based on a moving and scalable localizing Gaussian window [Stockwell *et al.*, 1996]. The width of this Gaussian window varies as a function of frequency along the time axis as it maps the 1-D time series into a complex function of both time and frequency [Mansinha *et al.*, 1997b]. A complete and lossless invertibility between the time (t) to time-frequency (t, f), to frequency (f) and back to time domain is achieved. The 1-D S-transform is defined as,

$$S(\tau, f) = \int_{-\infty}^{\infty} h(t) \frac{|f|}{\sqrt{2\pi}} e^{-\frac{(\tau-t)^2 f^2}{2}} e^{-i2\pi ft} dt \quad (1)$$

where $h(t)$ is the time series to be analyzed and τ is the time of the spectral localization. Note that the time average of $S(\tau, f)$ gives the Fourier spectrum.

[10] The 2-D S-transform provides variations in the amplitude of a time series for a particular period at each location. The 2-D S-transform is defined using,

$$S(x, y, k_x, k_y) = \int_{-\infty}^{\infty} \int_{-\infty}^{\infty} h(x', y') \frac{|k_x||k_y|}{2\pi} e^{-\frac{(x-x')^2 k_x^2 + (y-y')^2 k_y^2}{2}} \cdot e^{-i2\pi(k_x x' + k_y y')} dx' dy' \quad (2)$$

where x and y are spatial variables and k_x and k_y are wave-number variables ($k_x = 1/\lambda_x$, where λ_x is the wavelength in the respective direction).

3.3. Field Data Acquisition

[11] In November 2008, a 1.6 km long ruggedized SensorNet EnviroFlex FO cable (~ 1 cm diameter) with two 50-micron multimode fibers was installed on the riverbed at ~ 2 m from the river bank, about 0.15 to 0.76 m deep, approximately centered on the IFRC area (Figure 1). (Note that any use of trade, product, or firm names is for descriptive purposes only and does not imply endorsement by the U.S. Government). The cable was installed at 2 m from the river bank with the aim of capturing the connectivity between aquifer and the river. Heavy weights (large cobbles and/or breeze-blocks) were used to anchor the cable to ensure it remained static and under water. A Sensortran 8-channel Gemini control unit was programmed to collect the water temperature at the river bed every 0.51 m along the cable (for a total of 2871 measurement locations) at a 5 min interval. The FODTS system acquired data continuously for up to 6 mo at a time, with occasional down time used for system maintenance and re-calibration. In this study, we analyze two uninterrupted parts of the dataset with lengths of 19 and 30 d acquired during winter and summer months respectively. We are also analyzing the river stage data collected at 1 hr interval at ~ 1000 m from the IFRC area.

3.4. Time Series and Time-Frequency Analysis

[12] Time series analysis of FODTS data first focused on assessment of the temperature along the cable at different times of the year to identify likely zones of enhanced groundwater-surface water exchange. Time-series analysis was subsequently used to jointly interpret temperature time series and river stage time series in order to quantitatively evaluate how complex stage variations regulate exchange. Correlation coefficients were next calculated to evaluate the strength of the linear dependence between temperature and river stage time series for all spatial points along the river corridor.

[13] A 1-D S-transform was then used to describe the frequency content of the temperature signals at selected locations along the cable, in order to identify the periodic features present over the time series. Finally, we applied a 2-D S-transform to the temperature time series to acquire the space localized spectral (wavenumber) information at selected frequencies of interest as identified by the 1-D S-transform [Mansinha *et al.*, 1997b].

4. Results

[14] We first examine temperature variations along the cable at times of low river stage in the time series when the groundwater discharge into the river is expected to be strongest, due to the increase in the groundwater head. Groundwater discharge zones (GDZ) are identified as areas with both anomalously warm temperature in winter (Figure 1b, line 2) and anomalously cool temperature in the summer (Figure 1c, line 4). Such anomalies are only visible at low river stage (Figures 1b (line 2) and 1c (line 4)) and diminish at high river stage (Figures 1b (line 1) and 1c (line 3)). The locations of the anomalies are consistent in both winter and summer data.

[15] Figure 2 presents the relation between river stage and temperature for an exchange and a non-exchange zone. These locations are selected for analysis based on their proximity to the IFRC area and the fact that the zone of focused exchange coincides with a known uranium spring (Spr-9, Figure 2d) [Williams *et al.*, 2007]. The time series in the non-exchange zone (Figure 2a) shows a temperature

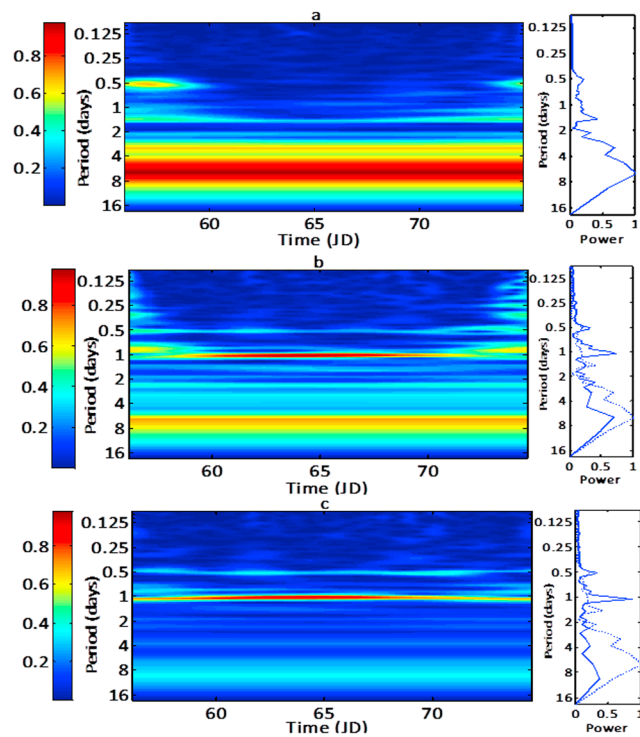


Figure 3. S-transform spectrum of time series for 19 d (27 February–16 March 2009). (a) S-transform of the river stage time series. (b) S-transform of the FODTS time series from a GDZ. (c) S-transform of the FODTS time series from a non-exchange zone. Plots on the right of the S-transform images represent the time averaged normalized power spectra (equivalent to the FFT), wherein the dashed lines are the river stage time average for comparison. Color bars display amplitude (power) linearly.

variation that is primarily driven by diurnal variation. Conversely, the temperature fluctuation in the GDZ (Figure 2b) shows a diurnal pattern with additional non-diurnal periods consistent with what might be inferred from the river stage data (Figure 2c). As expected, the difference in temperature is observed in Figure 2c when subtracting the temperature of the non-exchange zone from temperature of the exchange zone. The correlation coefficient between river stage and river water temperature along the cable provides more direct evidence of stage-controlled focused groundwater exchange along the river corridor. The temperature in the focused GDZ exhibits a weak negative correlation (~ -0.39 to -0.1) in the winter (Figure 2d, lines 1 and 2) and a strong positive correlation (~ 0.75 to 0.88) in the summer (Figure 2d, lines 3 and 4). Outside of the exchange zones, the correlation coefficient is relatively uniform, ~ 0.48 in the winter and ~ 0.7 in the summer. The sign of the correlation coefficient within GDZs is consistent with stage-driven groundwater discharge, as discussed below. Although there is a strong correlation outside of the GDZs, the sign of the correlation is inconsistent with stage driven groundwater discharge and instead likely results from stage driven variations in the amount of summer solar heating of the water column. Although the correlation coefficient offers a simple way to represent the control of stage on focused groundwater exchange, the relatively weak correlation in the winter data

(Figure 2d, line 2), along with the fact that much of the cable (away from the exchange locations) shows a strong correlation in the summer resulting from solar heating (Figure 2d, line 4), raises the need for less ambiguous measures of the mechanisms controlling the exchange—hence our consideration of the S-transform.

[16] Figure 3 shows the 1-D S-transform results of the river stage time series (Figure 3a), selected GDZ (Figure 3b) and a nearby non-exchange location (Figure 3c) (triangles in Figure 2). Short periods of 0.5 and 1 d characteristic of diurnal temperature variations are present in both GDZ and non-exchange zones. These are the only strong periods in the non-exchange area. In contrast, the strong amplitudes at longer periods (2–16 d) in the temperature data from the exchange area correspond well with the strong amplitudes observed at the same periods in the river stage data (Figures 3a and 3b). These periods are weak (period 7–15 d) or absent (period 2–7 d) in the non-exchange area (Figure 3c). These periodicities are also apparent in the time-averaged normalized power spectra (Fourier Spectrum) plots shown to the right of the S-transforms in Figure 3.

[17] The 2-D S-transform analysis of the entire FODTS dataset for three dominant periods (4, 1, and 0.5 d) identified in Figure 3 is shown in Figures 4b and 4c. The long-period behavior dominating the river stage (Figure 3a) is only evident in the zones of focused GDZ (Figure 4b, line 2). Other locations along the cable exhibit low amplitudes of ≤ 0.1 for the 4-d period. In contrast, the diurnal variations marked by short periods (0.5 and 1 d) are evident along the entire cable length (Figure 4c, lines 3 and 4).

5. Discussion

[18] FODTS of riverbed temperature along the Columbia River reveals the presence of focused groundwater exchange zones which likely facilitate the transfer of uranium from the aquifer to the river. Five identified exchange zones coincide with known uranium springs reported by *Williams et al.* [2007]. The relatively similar temperature recorded in the GDZs ($\sim 13^\circ\text{C}$ in the winter and $\sim 15^\circ\text{C}$ in the summer) is consistent with groundwater discharge during low river stage, as groundwater is known to have relatively constant temperature. The correlation coefficient between temperature and river stage provides a semi-quantitative link between groundwater discharge and river stage at the GDZs. The negative temperature-river stage correlation during winter results from discharge of warmer groundwater as the river stage falls. The positive temperature-river stage correlation during summer results from discharge of cooler water as the river stage falls. However, the high positive correlation between temperature and river stage in the non-exchange areas resulting from solar heating or seasonal changes highlights one limitation of relying on time series analysis of the stage-discharge relation alone for characterizing exchange. Furthermore, there are a few points on the cable where we see negative stage-discharge correlations in both the winter and summer data (Figure 2d, lines 2 and 4). These responses cannot be due to groundwater-surface water interaction.

[19] Time-frequency analysis of the FODTS data identified a distinct difference in the dominant periods of the temperature time series for the GDZ compared to a non-exchange area. Only diurnal variations in the temperature

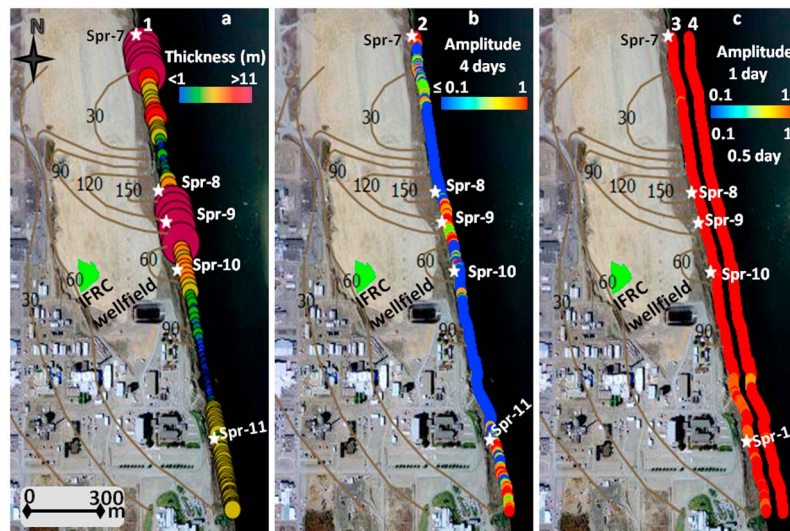


Figure 4. (a) Hanford Formation thickness as estimated from continuous waterborne electrical imaging measurements [Slater *et al.*, 2010] (line 1). White stars represent uranium seeps (Spr-7–Spr-11) [Williams *et al.*, 2007]. (b) Amplitude of period 4 d (line 2). (c) Amplitude of period 1 d (line 3) and amplitude of period 0.5 d (60 m offset) (line 4). Long periods shows strong signals in the exchange zones (thicker Hanford Formation), while we see effect of short periods (≤ 1 d) for the entire cable length. Brown contours in Figures 4a–4c show uranium concentration ($\mu\text{g/L}$) [Williams *et al.*, 2007]. All color scales are linear.

time series, marked by short periods of 1 d and 0.5 d appear in both exchange and non-exchange locations. Comparison of the S-transform for the river stage time series with the temperature time series shows that long period signals (≥ 2 d) dominating river stage time series are only present at the GDZ location (Figure 3). We argue that the amplitudes of these periods characterizing the stage-time series provide a more reliable indication of active stage-driven groundwater discharge relative to analysis of the stage-temperature correlation.

[20] The 2-D S-transform computed at these long periods (e.g., 4 d used here) captures information on spatial variability in the strength of the stage-driven groundwater discharge. High amplitudes at these long periods occur at locations along the river corridor (Figure 4b, line 2) corresponding to thicker Hanford Formation deposits (Figure 4a, line 1), possibly associated with buried channels incised into the Ringold Formation. Figure 4b (line 2) suggests that the zones of exchange may be more continuous than would be inferred using the stage-discharge correlation alone (Figure 2). A thicker Hanford Formation also coincides with the location close to the IFRC wellfield exhibiting high uranium concentration (Figure 4a) and identified GDZs (Figure 4b, line 2). The known uranium seeps reported by Williams *et al.* [2007] (Figures 4a and 4b) all coincide with high amplitudes zones in the 4 d period of the temperature time series identified with the 2-D S-transform. This is in contrast to the stage-discharge correlation results. For example, whereas Spr-8 (Figure 2d) would be interpreted as a non-exchange zone in the stage-discharge correlation plot, the 2-D S-transform identifies Spr-8 as a GDZ (Figures 4a (line 1) and 4b (line 2)). We therefore argue that time-frequency analysis provides a more reliable indication of where exchange is occurring compared to the stage-discharge correlation or temperature at low stage alone. The S-transform

analysis suggests that exchange is occurring more continuously along sections of the river corridor where the Hanford Formation is thickest. The 1-D S-transform analyses show that the long period signals related to groundwater-surface water exchange have a fairly uniform strength throughout the time series (unlike the 1 d and 0.5 d periods that are variable in strength). The variation in amplitude in 1 d and 0.5 d periods from 2-D S-transform analysis in Figure 4c) probably reflects variations in water depth and effect on solar heating. The time-frequency approach also allows us to effectively filter out all such diurnal effects and focus our interpretation on features in the time series associated with the salient periodicity of stage.

6. Conclusions

[21] We have demonstrated how the use of time-frequency analysis of FODTS time series can provide insights into the forcing mechanisms controlling groundwater-surface water exchange along a major river corridor. The time-frequency analysis using S-transform identified zones of contaminated groundwater discharge along a 1.6 km section of the Columbia River corridor and provided conclusive evidence of the stage-driven discharge associated with relatively long periods (≥ 2 d) in the river stage fluctuations. The correlation coefficient between river stage and temperature also identified spatial variability in exchange. However, linear correlation proved to be a less robust proxy indicator of groundwater discharge than the S-transform, as the river water temperature and hence correlation responds to variables other than the groundwater discharge alone. We conclude that time-frequency analysis is a powerful tool for improving understanding of dynamics of groundwater-surface water exchange from the spatially and temporally rich FODTS datasets.

[22] **Acknowledgments.** This research was supported by the U.S. Department of Energy under grant DOE - DE - FG02 - 08ER64561 with additional support from the U.S. Geological Survey Toxic Substances Hydrology Program. We thank Andy Ward, Christopher Strickland, and Jason Greenwood for field assistance. We are also grateful to Roelof Versteeg and Timothy Johnson for assistance with data storage and management.

[23] The Editor thanks the two anonymous reviewers for their assistance in evaluating this paper.

References

- Bechert, C. H., and J. M. Heckard (1966), Ground water, in *Natural Features of Indiana, 1816–1966: Sequecentennial Volume*, pp. 100–115, Indiana Acad. of Sci., Indianapolis.
- Constantz, J., L. C. Thomas, and G. Zellweger (1994), Influence of diurnal variations in stream temperature on streamflow loss and groundwater recharge, *Water Resour. Res.*, *30*(12), 3253–3264, doi:10.1029/94WR01968.
- Henderson, R. D., F. D. Day-Lewis, and C. F. Harvey (2009), Investigation of aquifer-estuary interaction using wavelet analysis of fiber-optic temperature data, *Geophys. Res. Lett.*, *36*, L06403, doi:10.1029/2008GL036926.
- Kunk, J. R., and S. M. Narbutovskih (1993), Phase I summary of surface geophysical studies in the 300-FF-5 operable unit, report, Westinghouse Hanford Co., Richland, Wash.
- Lindberg, J. W., and F. W. Bond (1979), Geohydrology and Groundwater quality beneath the 300 Area, Hanford site, *Rep. PNL-2949*, Pac. Northwest Lab., Richland, Wash.
- Lowry, C. S., J. F. Walker, R. J. Hunt, and M. P. Anderson (2007), Identifying spatial variability of groundwater discharge in a wetland stream using a distributed temperature sensor, *Water Resour. Res.*, *43*, W10408, doi:10.1029/2007WR006145.
- Ma, R., C. Zheng, M. Tonkin, and J. M. Zachara (2011), Importance of considering intraborehole flow in solute transport modeling under highly dynamic flow conditions, *J. Contam. Hydrol.*, *123*(1–2), 11–19, doi:10.1016/j.jconhyd.2010.12.001.
- Mansinha, L., R. Stockwell, R. Lowe, M. Eramian, and R. Schincariol (1997a), Local S-spectrum analysis of 1-D and 2-D data, *Phys. Earth Planet. Inter.*, *103*(3–4), 329–336, doi:10.1016/S0031-9201(97)00047-2.
- Mansinha, L., R. Stockwell, and R. Lowe (1997b), Pattern analysis with two-dimensional spectral localisation: Applications of two-dimensional S transforms, *Physica A*, *239*(1–3), 286–295, doi:10.1016/S0378-4371(96)00487-6.
- Newcomb, R. C. (1958), Ringold Formation of Pleistocene age in type locality, the White Bluffs, Washington, *Am. J. Sci.*, *256*, 328–340, doi:10.2475/ajs.256.5.328.
- Selker, J. S., L. Thévenaz, H. Huwald, A. Mallet, W. Luxemburg, N. van de Giesen, M. Stejskal, J. Zeman, M. Westhoff, and M. B. Parlange (2006a), Distributed fiber-optic temperature sensing for hydrologic systems, *Water Resour. Res.*, *42*, W12202, doi:10.1029/2006WR005326.
- Selker, J., N. van de Giesen, M. Westhoff, W. Luxemburg, and M. B. Parlange (2006b), Fiber optics opens window on stream dynamics, *Geophys. Res. Lett.*, *33*, L24401 doi:10.1029/2006GL027979.
- Slater, L. D., D. Ntarlagiannis, F. D. Day-Lewis, K. Mwakanyamale, R. J. Versteeg, A. Ward, C. Strickland, C. D. Johnson, and J. W. Lane (2010), Use of electrical imaging and distributed temperature sensing methods to characterize surface water–groundwater exchange regulating uranium transport at the Hanford 300 Area, Washington, *Water Resour. Res.*, *46*, W10533, doi:10.1029/2010WR009110.
- Stockwell, R. G., L. Mansinha, and R. P. Lowe (1996), Localization of the complex spectrum: The S-transform, *IEEE Trans. Signal Process.*, *44*(4), 998–1001, doi:10.1109/78.492555.
- Tyler, D. K. (1992), Assessment of potential environmental impacts from continued discharge to the 300 Area process trenches at Hanford, *Rep. WHC-SD-WM-EE-005*, Westinghouse Hanford Co., Richland, Wash.
- Williams, B. A., C. F. Brown, W. Um, M. J. Nimmons, R. E. Peterson, B. N. Bjornstad, D. C. Lanigan, R. J. Serne, F. A. Spane, and M. L. Rockhold (2007), Limited field investigation report for uranium contamination in the 300 Area, 300 FF-5 operable unit, Hanford site, Washington, *Rep. PNNL-16435*, Pac. Northwest Natl. Lab., Richland, Wash.
- F. Day-Lewis and C. Johnson, Branch of Geophysics, Office of Groundwater, U.S. Geological Survey, 11 Sherman Pl., Unit 5015, Storrs, CT 06269, USA.
- M. Elwaseif, K. Mwakanyamale, and L. Slater, Department of Earth and Environmental Sciences, Rutgers University, 101 Warren St., Newark, NJ 07102, USA. (kisam@pegasus.rutgers.edu)